Hindawi
Advances in Civil Engineering
Volume 2022, Article ID 6071868, 14 pages
https://doi.org/10.1155/2022/6071868

Research Article

Numerical Analysis of the Influence of Deep Foundation Pit Construction on Adjacent Subway Stations in Soft Soil Areas

Tao Yang, Shengyuan Xiong, Shuailei Liu, Yang Liu, Hao Zhao, and Yanwei Li

School of Urban Planning and Municipal Engineering, Xi'an Polytechnic University, Xi'an, Shaanxi 710048, China

Correspondence should be addressed to Tao Yang; yangtao@xpu.edu.cn

Received 16 February 2022; Revised 10 March 2022; Accepted 23 March 2022; Published 5 April 2022

Academic Editor: Yuan Mei

Deep foundation pit construction adjacent to a subway station in a soft soil area was numerically simulated with Midas GTS NX calculation software. The influence of the deep foundation pit construction on the deformation and stress of the subway station structure was studied, and the influence of the foundation pit retaining structure on the station was analyzed. The results show that during the foundation pit excavation process, the subway station slab rose as a whole and was greatly affected by the deformation of the common ground connecting wall, with the most unfavorable position changing as the excavation area changed. The excavation of foundation pits in different zones had a considerable influence on the east-to-west displacement of the common diaphragm wall outside the foundation pit. The maximum positive bending moment of the common diaphragm wall changed little, while the negative bending moment increased greatly during construction. Overall, the foundation pit excavation had a great impact on the negative moment of the common diaphragm wall. During the foundation pit excavation process, the subway station column lifted upward, and the maximum displacement, which was located at the west end of the station near the foundation pit, gradually weakened from west to east. As the foundation pit excavation process continued, the maximum axial force of the station column increased by 10.38%, and the pressure was the largest in the middle column. As the thickness of the diaphragm wall increased, the stiffness of the foundation pit retaining structure increased. After earthwork excavation and unloading, the locations in the retaining structure with high stiffnesses could resist deformations. The whole foundation pit was offset due to the high stiffness of the foundation pit retaining structure, which increased the horizontal deformation of the existing station structure. With increasing thickness, the relative horizontal deformation of the station slab gradually increased, mainly because the difference between the depths of the old and new diaphragm walls caused the embedded soil of the two same deep foundation pits to differ. Furthermore, there were great differences in the Earth pressure behind the wall. As the depth of the diaphragm wall increased, the active Earth pressure behind the diaphragm wall increased.

1. Introduction

As urban underground space and rail transit have rapidly developed, commercial and civil construction along subway lines have increased, resulting in building foundation pits becoming increasingly closer to subway stations [1]. When the soil inside a deep foundation pit is excavated, the soil stress is redistributed, and the pressure on both sides of the retaining structure becomes unbalanced, resulting in the displacement of the retaining structure inside the foundation pit, which produces additional stress on adjacent subway structures, causing the subway structure to deform and affecting the safe operation of the subway [2]. In recent years, many scholars have studied disturbances caused by foundation pit excavation in soft soil areas with numerical simulations. As an example, Jian et al. [3] used finite element analysis software and actual monitoring results from a foundation pit project to propose a generalized curve for the ground settlement behind a foundation pit support structure in a soft soil area, and they developed an applicable formula for the lateral deformation of the support structure and the ground settlement. Sun [4] used finite element analysis software to simulate the influence of deep foundation pit excavation on adjacent subway stations, and they analyzed the stress of deep foundation pit retaining structures and studied the internal force and deformation of subway

stations. Wang et al. [5] used ABAQUS software to study the deformation characteristics of an existing subway station by excavating on both sides of a deep foundation pit. The results showed that symmetrical excavation was beneficial for controlling the horizontal displacement of the subway station, while asymmetric excavation was beneficial for controlling the vertical displacement of the station. Guo et al. [6] simulated the deformation of a common diaphragm wall foundation pit during subway station transfer with ABAQUS software. In contrast to the deformation of ordinary retaining structures without underground structures, the deformation of the underground diaphragm walls in common sections was small above the foundation pit excavation surface, with the greatest lateral deformation occurring 8 m below the excavation surface.

There are few reports on the deformation mechanisms of deep foundation pit construction adjacent to subway stations in existing research. With an increasing number of underground diaphragm walls shared by subway stations and foundation pits, determining the stress change in the surrounding soil due to deep foundation pit excavation and the deformation mechanism of common wall subway stations due to changes in soil stress are major tasks, as well as a source of concern for many scholars [7, 8]. Based on a deep foundation pit project in Suzhou and simulations of different subway station structures, this paper explores the deformation relationship and internal force action mechanism of adjacent subway stations caused by deep foundation pit excavation to provide a reference for relevant projects.

2. Project Introduction

2.1. Project Profile. In a station foundation pit project in Suzhou, the total length of the foundation pit was 407.1 m, the excavation width of the standard section was 20.35 m, and the width of the docking expansion section near the end of metro line S3 was 41.7 m. The excavation depth of the station basement was 17~19 m, and the thickness of the roof soil was approximately 2.9~3.5 m. The whole foundation pit was constructed by the open-cut method. To avoid disrupting traffic, a temporary pavement system was built along Yiting Road and the S3 line, and semicover excavation was carried out. In this foundation pit, two sealing walls were installed, dividing the foundation pit into three sections. A schematic diagram of the foundation pit is shown in Figure 1.

2.2. Geological Conditions. The proposed site was located in a low-terrain region of the Tai Hu Basin, in the lower reaches of the Yangtze River. The foundation soil from the surface to a depth of approximately 70.0 m consists of loose sediments deposited from the Quaternary Holocene to the early Pleistocene era, mainly clay soil and interbedded sandy soil. The physical and mechanical parameters of the soil layer are shown in Table 1. The groundwater at the site was divided into three categories based on the occurrence condition: groundwater in the shallow filling layer, with a stable water level of 0.51~0.90 m; microconfined water in the ③$_3$ silt layer and ④$_2$ silt sand layer, with a stable water level of 0.50~0.60 m; and confined water in the ⑦$_2$ silt sand layer, with a stable water level of −2.50 to −2.80 m and an annual variation of approximately 1 m.

2.3. Foundation Pit Excavation and Enclosure Scheme. The station foundation pit was constructed by section, and the foundation pits in areas B and C at both ends were preferentially excavated. The foundation pit in area A, which was close to the station of metro line S3 and had the longest excavation length, was not initially excavated. After the integral support structures were constructed in areas B and C, the foundation pit in area A was excavated. As a result, the support stiffness of the S3 subway station was increased and the foundation pit excavation length was decreased, effectively reducing the influence of the narrow and long foundation pit excavation on the S3 subway structure and minimizing the influence of soil unloading on the S3 subway station, reducing the construction risk. The construction was carried out in strict accordance with the principle of "support before excavation, limited time support, layered excavation, and no over excavation" to minimize the exposure time and area of the foundation pit without support. Figure 2 shows a sectional construction drawing of the station foundation pit.

Given the deep foundation pit excavation, poor geological conditions, and high safety risks, an 800 mm thick diaphragm wall and an internal support enclosure scheme were designed. The length of the designed ground wall in the standard section was 29.5 m, the length of the end ground wall was 32.5 m, the length of the continuous wall under the cover was 30.64 m, and the total length of the enclosure structure completed in one week was 783 m. The inner support included both concrete support and steel support, with a section size of 800 mm × 1000 mm for the concrete support and a section diameter of 609 mm for the steel support. The excavation of the foundation pit inevitably disrupted the surrounding environment. To ensure the protection of the S3 line during construction, eight MJS (Metro Jet System) piles were set in the joint of the common ground wall for water-stop reinforcement.

3. Foundation Pit Excavation Simulation

3.1. Model Establishment. After consulting a large number of papers on numerical simulations of foundation pit excavations, the modified Mohr–Coulomb model was adopted, and Midas GTS NX software was used to simulate the project. The modified Mohr–Coulomb model was adjusted based on the Mohr–Coulomb constitutive model. This model is essentially a combination of a nonlinear elastic model and an elastic-plastic model. It is commonly used to simulate silt and sand. The modified Mohrs–Coulomb model can simulate double hardening behavior, which is not affected by shear failure or compressive yield. Table 2 shows the soil layer and structural calculation parameters.

According to the Saint-Venant principle, deformation and settlement effects at distances larger than three times the

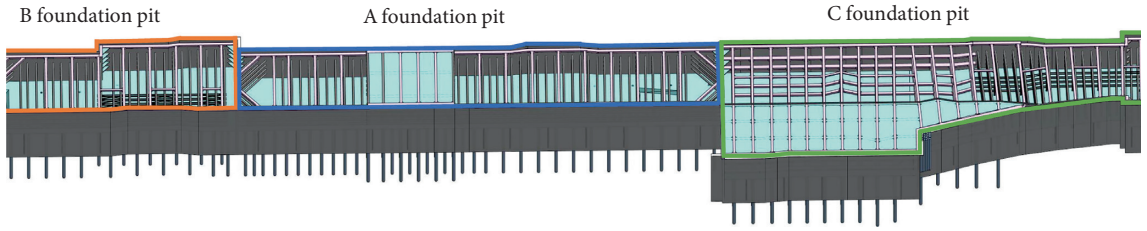

Figure 1: Schematic diagram of a foundation pit.

Table 1: Physical and mechanical parameters of the soil layer.

Soil horizon	Moisture content W (%)	Specific gravity (G_s)	Force of cohesion C (kPa)	Internal friction angle ϕ/°	Modulus of compression E_s (MPa)
①$_3$ plain fill	32.0	2.73	15	12	—
③$_1$ clay	26.9	2.74	43.0	15.5	8.10
③$_2$ silty clay	29.8	2.73	25.5	12.1	6.91
③$_3$ silt	28.6	2.69	6.0	25.4	10.69
④$_2$ sand with silt	26.3	2.69	3.8	31.8	12.50
⑤$_1$ silty clay	30.2	2.73	29.8	14.3	6.01
⑥$_1$ clay	25.8	2.74	54.9	16.1	8.36
⑥$_2$ silty clay	28.5	2.73	29.7	13.8	6.41
⑦$_1$ silty clay	31.6	2.72	27.6	15.0	5.32
⑦$_2$ silty soil with silt	28.6	2.70	10.8	23.4	9.45

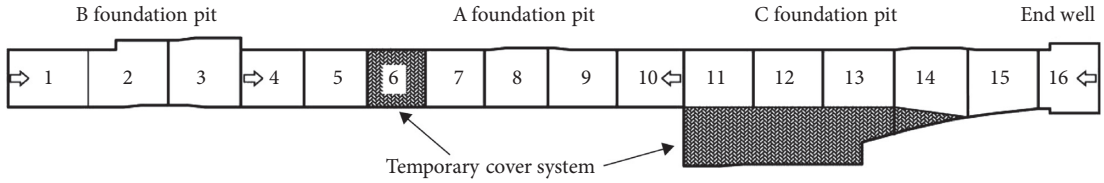

Figure 2: Sectional construction drawing of the station foundation pit.

Table 2: Soil layer and structural parameters.

Soil layer and structural	μ	C (kPa)	ϕ/°	Material type	γ (kN/m^3)	K_0	E_s/(MPa)
①$_3$ plain fill	0.43	15.0	12.0	—	18.62	0.75	—
③$_1$ clay	0.32	43.0	15.5	—	19.40	0.48	8.10
③$_2$ silty clay	0.33	25.5	12.1	—	18.91	0.50	6.91
③$_3$ silt	0.30	6.0	25.4	—	18.62	0.43	10.69
④$_2$ sand with silt	0.29	3.8	31.8	—	19.01	0.41	12.50
⑤$_1$ silty clay	0.33	29.8	14.3	—	18.91	0.50	6.01
⑥$_1$ clay	0.31	54.9	16.1	—	19.70	0.45	8.36
⑥$_2$ silty clay	0.32	29.7	13.8	—	19.21	0.47	6.41
⑦$_1$ silty clay	0.35	27.6	15.0	—	18.72	0.53	5.32
⑦$_2$ silty soil with silt	0.31	10.8	23.4	—	18.82	0.44	9.45
Crown beam	0.2	—	—	C35	25	—	30000
Underground continuous wall	0.2	—	—	C35	25	—	30000
Surrounding	0.3	—	—	Q235	78	—	210000
Concrete support	0.2	—	—	C35	25	—	30000
Steel support	0.3	—	—	Q235	78	—	210000

excavation edge of the deep foundation pit are small and can be ignored. When this result was combined with provisions in the technical code for construction safety in the Building Deep Foundation Pit Engineering (JGJ311-2013) [9], the range $0.7H$ or $H{\cdot}\tan(45^\circ{-}\varphi/2)$ from the edge of deep foundation pit was determined to be the most important influence area; the secondary influence areas were $0.7H$~(2.0~3.0) H or $H{\cdot}\tan(45^\circ{-}\varphi/2)$~(2.0~3.0) H around deep foundation pit, where H is the design depth of the deep foundation pit (m), as shown in Figure 3. In summary, a

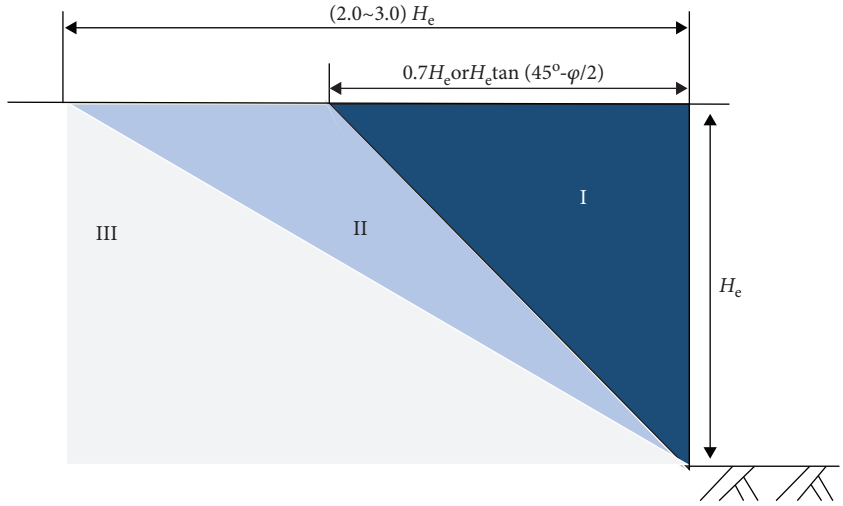

Figure 3: Impact zone of deep foundation pit engineering.

reasonable overall model size was selected based on the size of the deep foundation pit excavation in practical engineering, improving the calculation speed and the presentation of the numerical simulation results. The boundary value in the model was 510 m × 150 m × 60 m.

3.2. Construction Procedures. Midas GTS/NX software was used to simulate the dynamic construction process by activating or passivating the grid group. Deep foundation pit engineering includes the construction of long, narrow, deep foundation pits. Thus, the excavation must be completed in stages. Without changing the construction method, the construction steps were appropriately simplified, as shown in Table 3.

4. Finite Element Calculation Results

In the foundation pit excavation process, the deformation and internal force changes adjacent to the station are important guides for engineering construction. The excavated foundation pit shared a 274.5 m ground connecting wall with a station of line S3, which necessitated complex construction, a large project scale, and many construction steps. Therefore, representative working condition steps were selected for detailed analysis, such as working condition 8 (construction of the bottom plate), working condition 14 (middle stage of the excavation), and working condition 20 (backfilling and covering soil). The influence of the soft soil deep foundation pit excavation on the deformation and internal forces of the floor slab, common wall, and bearing column near the subway station were analyzed with finite element simulation in this section.

4.1. Analysis of the Deformation and Internal Force of the Station Floor Slab Caused by Excavation. Figure 4 shows the deformation of the subway station floor after each zone was excavated. Under working condition 8, the station slab of the noncommon ground wall section and common ground wall section in areas A and C tended to deform outside the foundation pit, with a maximum deformation of −1.95 mm for the overhead slab at the west end of the station. Near the excavation area in area B, the station slab deformed into the foundation pit, with a maximum deformation of 3.96 mm mainly concentrated at the bottom slab. Under working condition 14, the displacement outside the foundation pit adjacent to excavation area C was large, with a maximum deformation of −3.18 mm. The deformation trend of the station slab was consistent with that under working condition 8, with a maximum deformation of 4.31 mm near area B. Under working condition 20, the horizontal displacement of the station floor near areas A and B was large, with a maximum deformation of 5.42 mm. The horizontal deformation of the station slab showed a differential deformation trend of overall deformation inside the foundation pit and local deformation outside the foundation pit. The vertical deformation of the station slab showed a differential deformation trend of overall upward uplift and local downward settlement, with a maximum differential displacement of 8.51 mm, ensuring that the station structure can be used normally. The vertical deformation of the station slab was greatly affected by the heave and subsidence of the common ground wall. The deformation of each layer of the slab was consistent, with the maximum deformation mainly concentrated on the side of the common ground wall. As the excavation progressed, the maximum vertical deformation of the station slab successively occurred at the common ground connecting wall in areas B, C, and A, with values of 5.44 mm, 5.82 mm, and 8.30 mm, respectively. In addition, the maximum vertical displacement of the station slab was much larger than its horizontal displacement. The author believes that foundation pit excavation has a smaller impact on the horizontal direction of the station slab than on the vertical direction of the station slab. The station slab mainly produced uplift deformation and was prone to large vertical displacements due to the joint action of the uplift at the bottom of the foundation pit [10].

During the foundation pit construction process, the soil stress is redistributed, and the internal force of the existing station structure changes accordingly [11]. To further

Table 3: Key construction steps.

Working condition		Construction stage	Excavation depth (m)
1		Balance in-situ stress, building additional stress simulation, displacement clearing	—
2		Construction of diaphragm wall, column and temporary pavement system	—
3		Excavate the first layer of soil as the first concrete support	1.64
4		Excavate the second layer of soil and erect the second steel support	5.04
5		Excavate the third layer of soil and erect the third layer of steel support	7.94
6		Excavate the fourth layer of soil and erect the fourth steel support	10.84
7	Area B	Excavate the fifth layer of soil and erect the fifth steel support	13.74
8		Excavate the sixth layer of soil and construct the bottom plate	17.21
9		Remove the 4th and 5th steel supports, construct side walls and middle plates	—
10		Remove the second and third steel supports, construct side walls and top plates	—
11		Remove the first concrete support and backfill the covering soil	—
12		Excavate the first layer of soil as the first concrete support	1.64
13		Excavate the second layer of soil and erect the second steel support	5.04
14		Excavate the third layer of soil and erect the third layer of steel support	7.94
15		Excavate the fourth layer of soil and erect the fourth steel support	10.84
16	Area C	Excavate the fifth layer of soil and erect the fifth steel support	13.74
17		Excavate the sixth layer of soil and construct the bottom plate	17.21
18		Remove the 4th and 5th steel supports, construct side walls and middle plates	—
19		Remove the second and third steel supports, construct side walls and top plates	—
20		Remove the first concrete support and backfill the covering soil	—
21		Excavate the first layer of soil as the first concrete support	1.64
22		Excavate the second layer of soil and erect the second steel support	5.04
23		Excavate the third layer of soil and erect the third layer of steel support	7.94
24		Excavate the fourth layer of soil and erect the fourth steel support	10.84
25	Area A	Excavate the fifth layer of soil and erect the fifth steel support	13.74
26		Excavate the 6th layer of soil, construct the bottom plate, remove the blocking wall	17.21
27		Remove the 4th and 5th steel supports, construct side walls and middle plates	—
28		Remove the second and third steel supports, construct side walls and top plates	—
29		Remove the first concrete support and backfill the covering soil	—

explore the impact of an excavated deep foundation pit that shares a continuous wall with an existing station on the internal force of the station slab, Figure 5 shows the bending moment cloud diagram of the subway station slab during foundation pit excavation, and Figure 6 shows the maximum bending moment of each layer of the station slab during foundation pit excavation. According to the analysis in Figure 5, a negative bending moment occurred near the bottom plate of the subway station and at the beam-column joints, while a positive bending moment occurred in the middle of the plate. The bending moment was generally higher in the Y direction than in the X direction, with an average difference of 392.18 kN ∗ m. As construction progressed, the maximum bending moments of the station bottom plate were −2725.41 kN ∗ m, −2664.01 kN ∗ m, and −2740.99 kN ∗ m in areas A, B, and C, respectively, and were mainly distributed at the connection between the bottom plate and the sidewall opposite the foundation pit. The maximum positive bending moment was generally greater in the X direction than in the Y direction, with an average difference between the extreme values of 142.05 kN ∗ m. In contrast, the maximum negative bending moment was generally greater in the Y direction than in the X direction, with an average difference between the extreme values of 179.42 kN ∗ m. Under different working conditions, the bending moment changed little in the two directions of the station slab, and the excavation of the foundation pit had only a minor impact on the internal force of the adjacent station slab. The maximum bending moment of the bottom slab did not vary across different zones, and the bending moment distribution in the same direction was consistent. There were more positive bending moments in the Y direction and less positive bending moments in the X direction near the foundation pit.

4.2. Analysis of the Deformation and Internal Force of the Station Common Wall Caused by Foundation Pit Excavations. The common diaphragm wall is closely related to the outer wall of the existing subway station, and the two change approximately in coordination [12]. The deformation of the common diaphragm wall has a considerable effect on the deformation of the existing subway station [8]. Therefore, it is essential to explore the deformation and stress of the common diaphragm wall.

Figures 7 and 8 show the deformation nephogram of the horizontal deformation of the common diaphragm wall in area B in the east-west direction and north-south direction after excavating each partition. According to Figure 8, the deformation trend of the common diaphragm wall is similar to that of the station wall. After excavating the foundation pit in area B, the common diaphragm wall as a whole exhibited a deformation trend toward the foundation pit. The maximum displacement was 9.30 mm in the middle and lower parts of the adjacent excavation area, and the upper wall of the foundation pit near area A exhibited a deformation trend

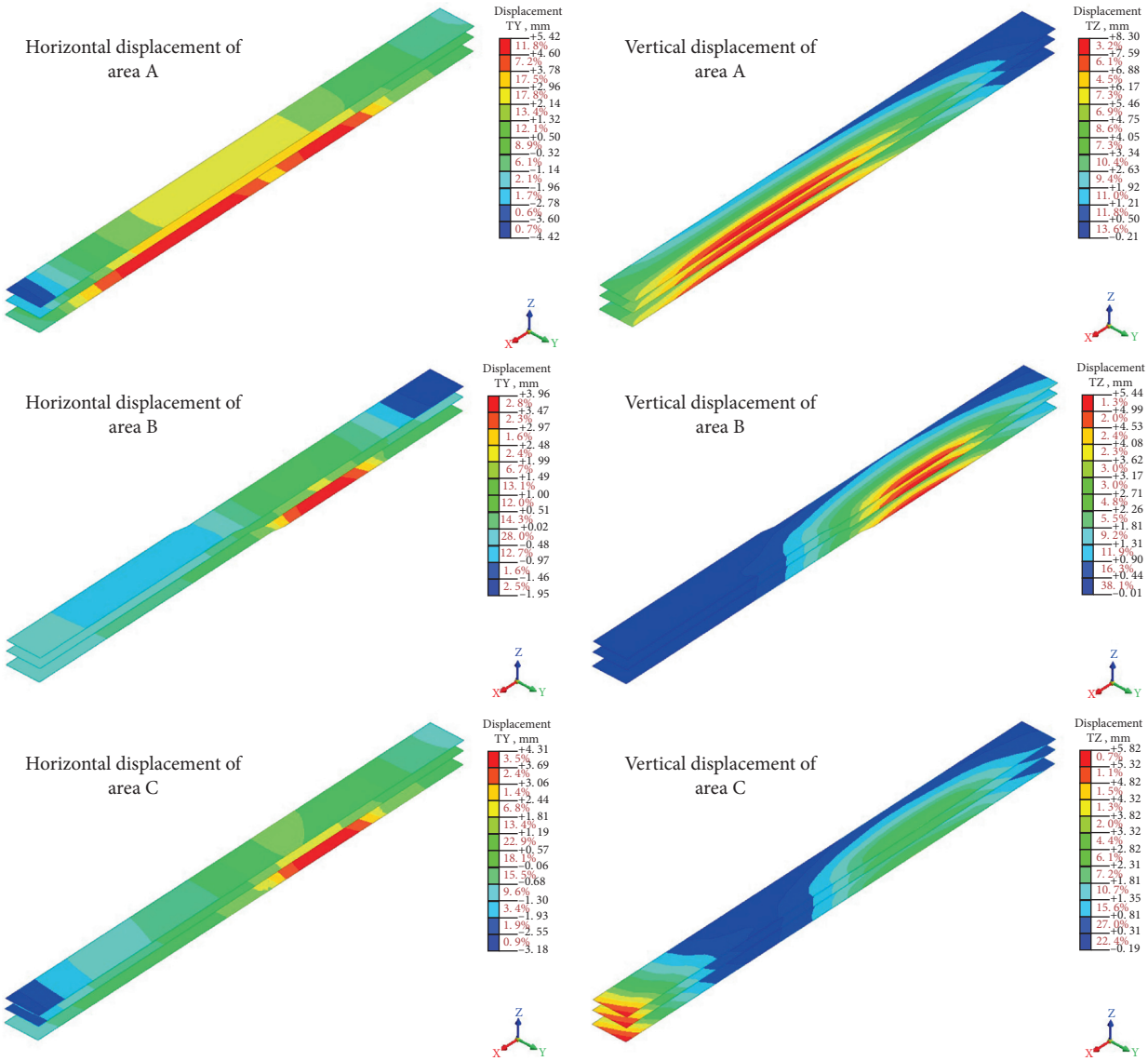

Figure 4: Horizontal and vertical displacements due to foundation pit excavation in the pit bottom station of each area.

toward the outside of the foundation pit, with a maximum deformation of −2.46 mm. After excavating the foundation pit in area C, the maximum displacement and position of the common ground connecting wall did not change, and the maximum displacement was 9.38 mm. The displacement outside the foundation pit was transferred from the upper wall of the foundation pit in area A to the middle and upper parts of the common ground connecting wall in the foundation pit excavation area, and the maximum deformation was −3.44 mm. After excavating the foundation pit in area A, the displacement of the middle and upper parts of the common ground connecting wall adjacent to area C with the outside of the foundation pit increased to −5.06 mm. At the same time, the deformation of the common diaphragm wall in the middle and lower parts of adjacent areas A and B increased, with a maximum deformation of 9.95 mm in the common diaphragm wall in the middle and lower parts of in area A. The excavation of the foundation pit in different zones had a considerable influence on the displacement of the east-west common diaphragm wall outside the foundation pit.

As shown in Figure 9, after excavating the foundation pit in area B, the maximum deformation occurred at the lower left part of the common diaphragm wall, with a maximum displacement of −0.13 mm. There was a small deformation section outside the foundation pit in the upper right part of the common diaphragm wall, with a maximum value of −0.47 mm. After excavating the foundation pit in area C, the deformation trend of the common diaphragm wall in the north-south direction was symmetrical with that after excavating the foundation pit in area B. The displacement was the largest at the lower left part of the common diaphragm wall, with a maximum value of 6.57 mm, while the deformation outside the foundation pit in the smaller section at the upper left part of the common diaphragm wall was only −5.05 mm. After excavating the foundation pit in area A, the

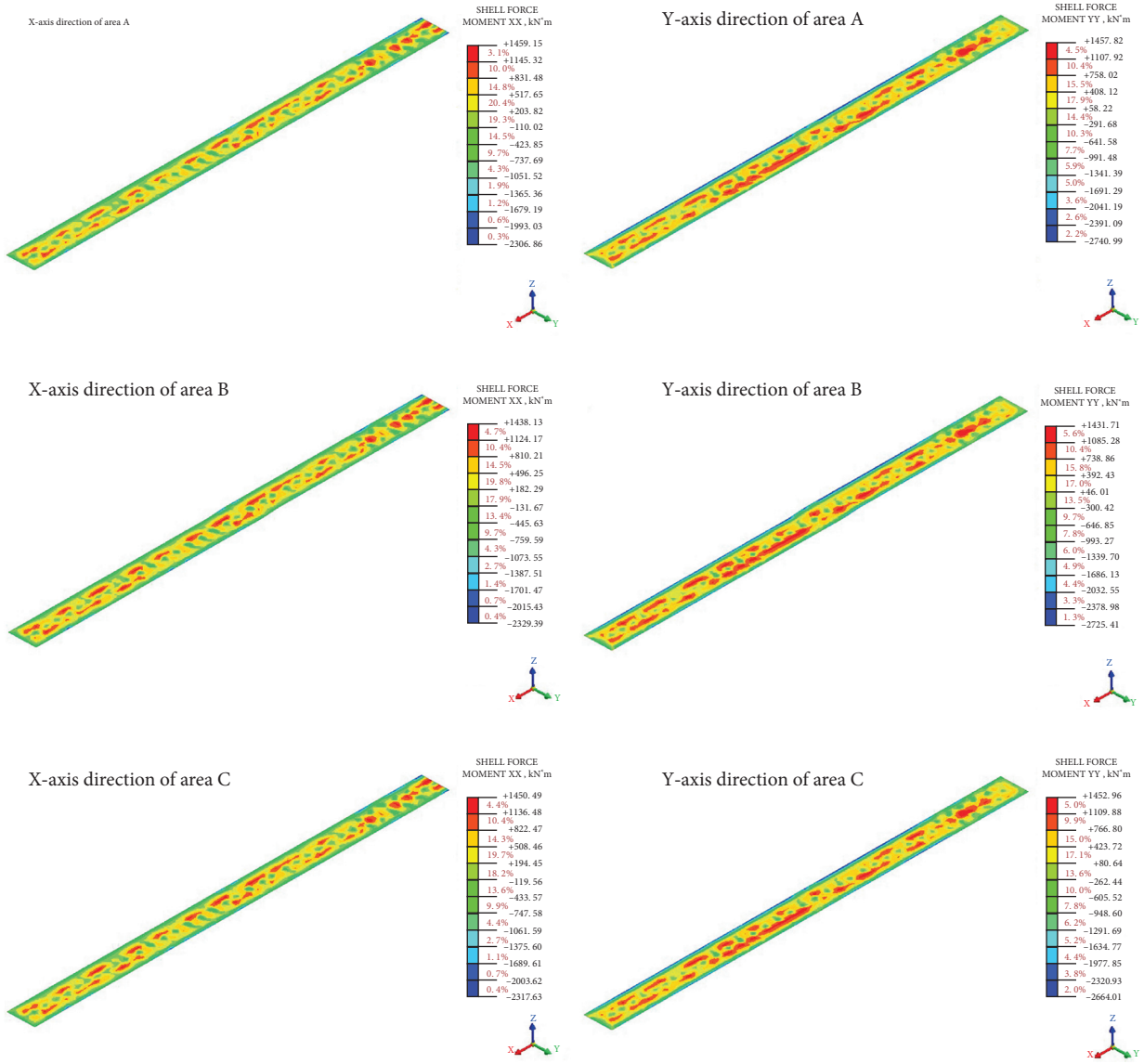

Figure 5: Distribution of bending moments in the X and Y axes from the foundation pit excavation to the station bottom plate in each area.

overall change trend was the same as that in area C, but the overall deformation was slower. The maximum displacement of the inside of the foundation pit was 2.25 mm, and the maximum displacement of the outside of the foundation pit was −3.75 mm. Based on the above analysis, the excavation of the foundation pit in area B had little impact on the north-south common diaphragm wall, mainly because area B was far from the influence area of the foundation pit. The excavation of the foundation pit in area A greatly reduced the deformation of the common diaphragm wall in the north-south direction, mainly because the excavation of the foundation pit in area A caused the common diaphragm wall to deform in the east-west direction in the foundation pit, decreasing the normal upward deformation of the common diaphragm wall in the north-south direction.

Figures 9 and 10 show the vertical deformation distribution and maximum bending moment of the common diaphragm wall before and after foundation pit excavation. Under working condition 8, the bending moment of the common underground diaphragm wall in the X direction was generally negative and small. The maximum bending moment at the junction of the partition wall in areas B and C and the bottom plate of the existing underground station was 523.75 kN ∗ m, with the minimum bending moment occurring below the bottom plate. The positive bending moment was concentrated in the middle and lower parts of the common diaphragm wall near the foundation pit in area B. The bending moment of the common diaphragm wall in the Y direction was dominated by the positive bending moment; the positive bending moment occurred above the station floor, while the negative bending moment occurred below the floor and near the partition wall and was slightly larger than the bending moment in the X direction. Under working condition 14, the bending moment distribution of the common diaphragm wall in the X direction was similar to that under working condition 8, whereas the bending

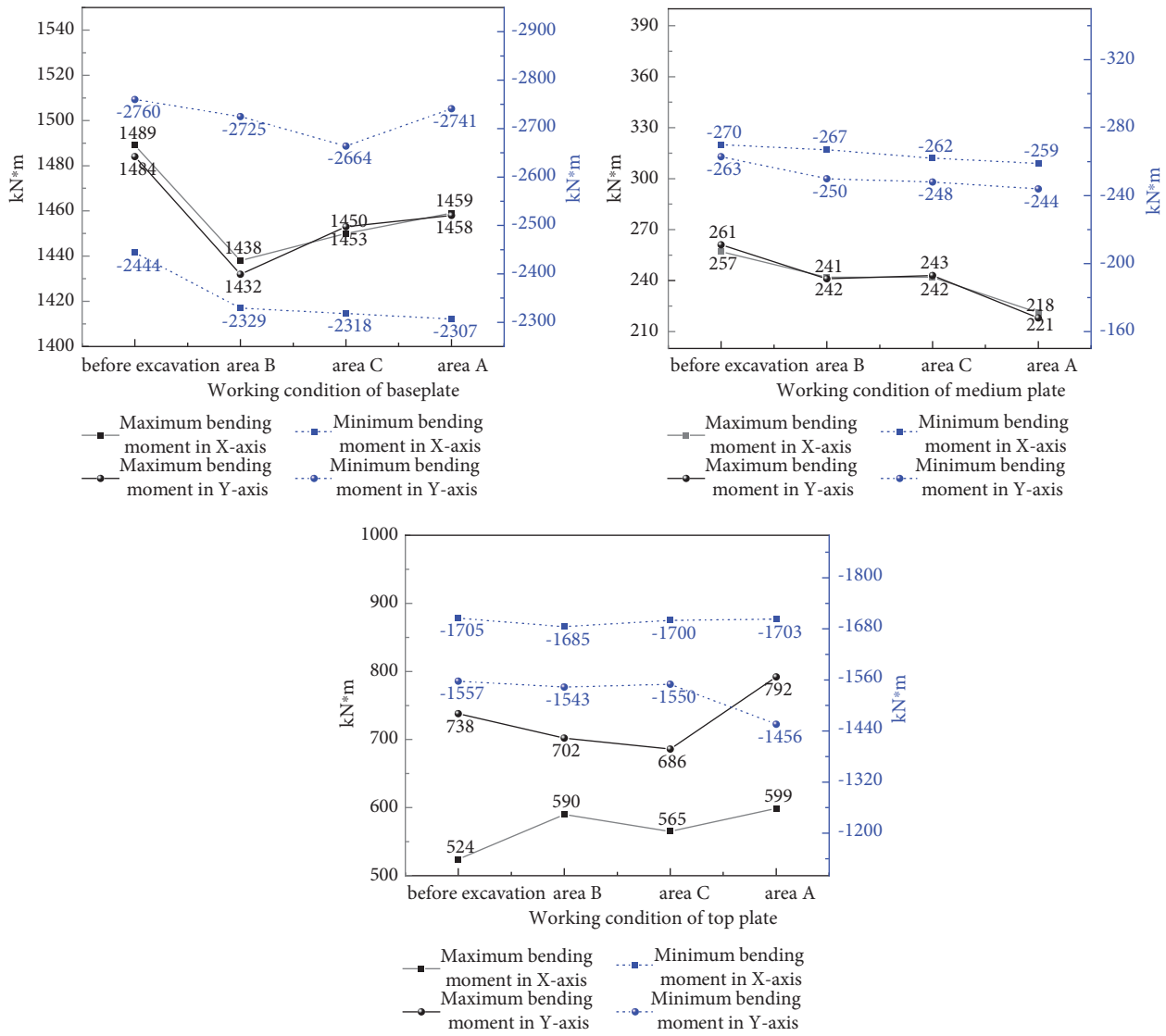

Figure 6: Maximum bending moment of the station slab from the foundation pit excavation to the pit bottom.

moment distribution of the common diaphragm wall in the *Y* direction was thinner than that under condition 8. Under condition 20, due to the influence of soil unloading, the strip positive bending moment appeared in the foundation pit excavation area and the station floor area in area A. During excavation, the maximum positive bending moment of the common diaphragm wall changed little, whereas the negative bending moment increased greatly. Compared with condition 8, the negative bending moments in the *X* direction and *Y* direction increased by 10.18% and 21.08%, respectively, under condition 14. The negative bending moment in the *X* direction under condition 20 was 12.74% larger than that under condition 14, but the change in the negative bending moment in the *Y* direction was small. Before and after excavation, the common diaphragm wall changed greatly. The positive bending moment in the *X* direction increased by 35.29% and the negative bending moment increased by 99.71%. The positive bending moment in the *Y* direction increased by 22.26% and the negative bending moment increased by 64.44%. Overall, foundation pit excavation has a considerable impact on the negative bending moment of the common diaphragm wall. In the design of similar projects, the negative reinforcement configuration of the common diaphragm wall should be considered [13].

4.3. Analysis of the Deformation and Internal Force of the Station Column Caused by Foundation Pit Excavation. Figure 11 shows the vertical deformation distributions of the subway station column before and after foundation pit excavation. Overall, the station column exhibited uplift deformation. Under working condition 8, the uplift deformation of the station column was relatively large near the foundation pit in area B, with a maximum deformation of 2.75 mm extending to both ends. The uplift deformation decreased gradually, with the smallest uplift deformation at the west end. Under working condition 14, only the station

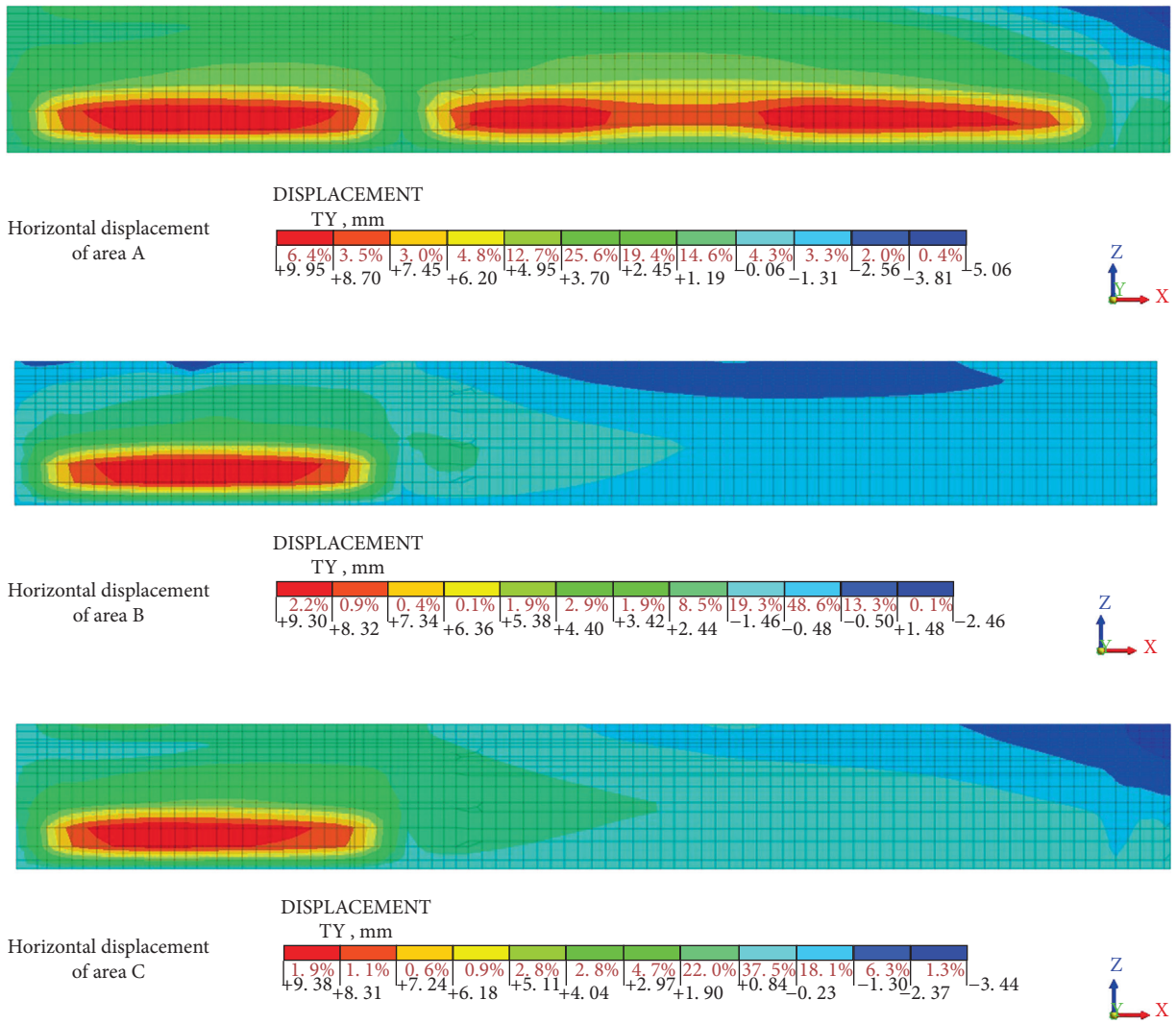

Figure 7: Deformation cloud diagram of the horizontal deformation of the common diaphragm wall in the east-west direction after excavating each partition.

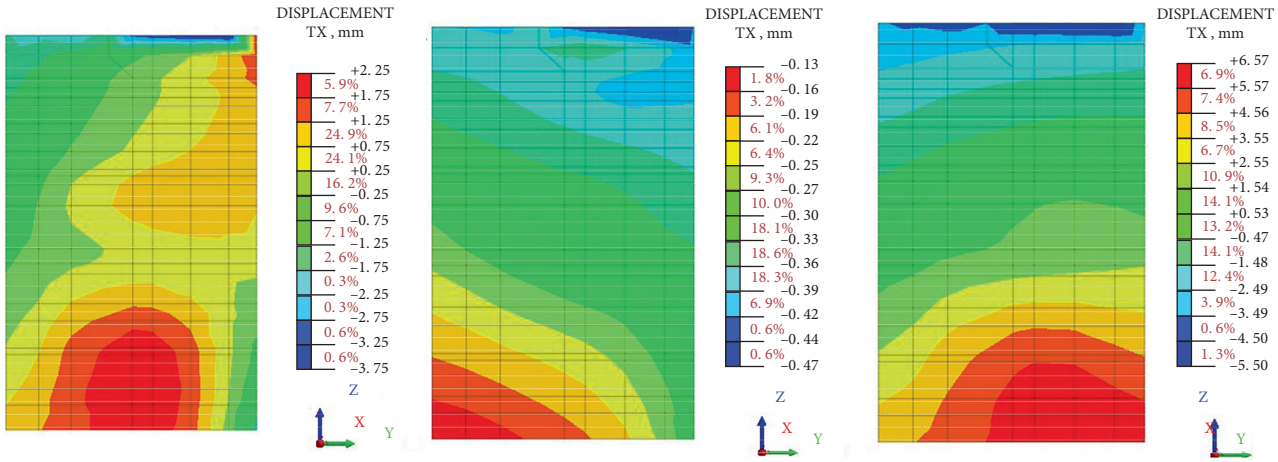

Figure 8: Horizontal displacement of the common ground wall in the north-south direction when the foundation pit in area B was excavated to the pit bottom.

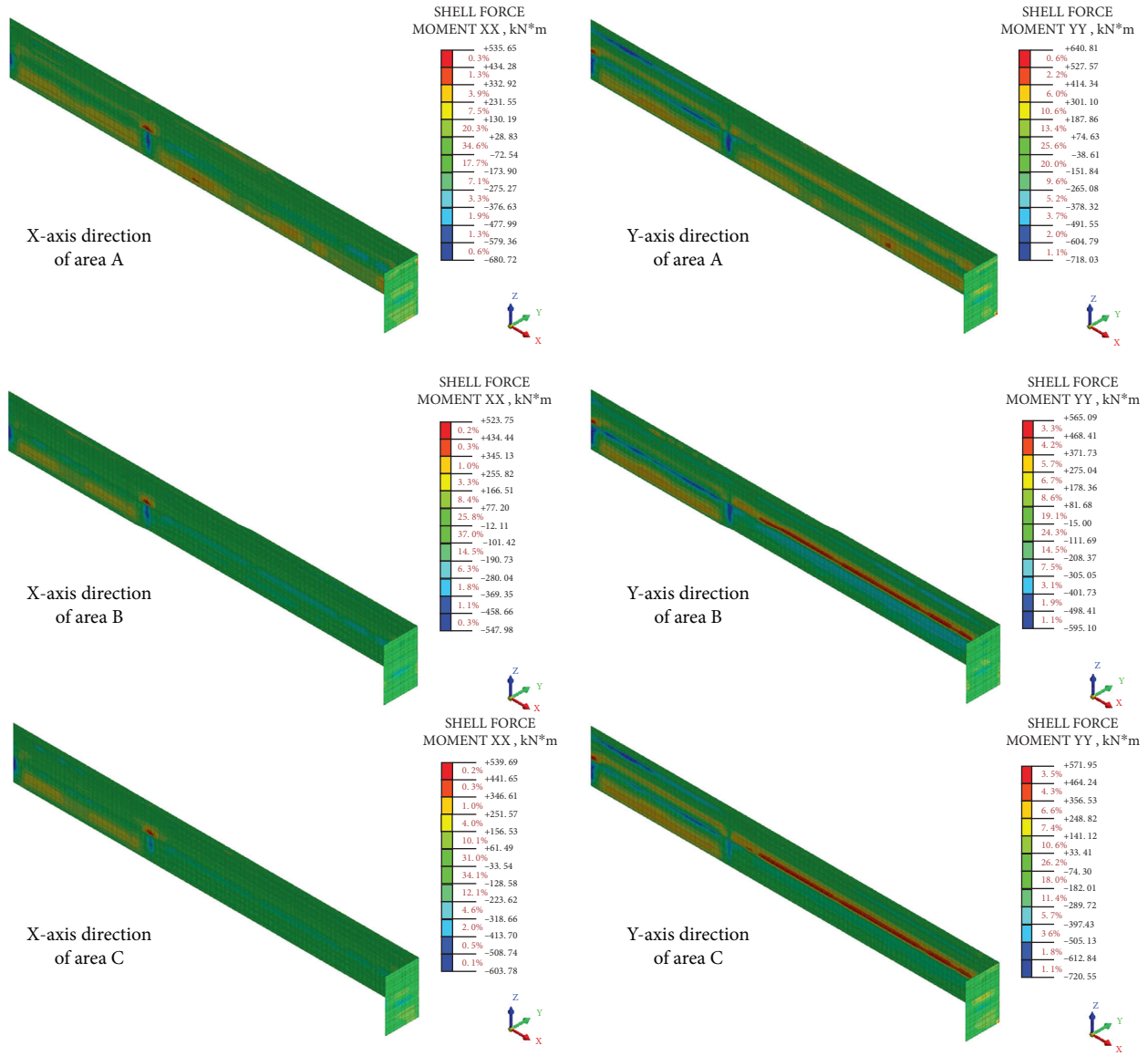

Figure 9: Bending moment distribution along the X and Y axes of the common ground wall from the foundation pit excavation to the pit bottom in each area.

column adjacent to the common ground wall had a large uplift, and the maximum deformation was 5.15 mm. The deformation far from the foundation pit excavation area was small, but the station column near the foundation pit in area B collapsed, showing a maximum deformation of 1.78 mm, which was 35% less than that before foundation pit excavation. Under working condition 20, due to the excavation of the foundation pit in area A, the deformation of the columns in the west end of the station is large, with a maximum deformation of 4.53 mm at the west end. From west to east, the uplift of the station gradually decreased. The differential settlement between the columns caused additional stress in the structure, which may lead to structural cracking and damage. Therefore, the differential settlement between the columns should be considered during foundation pit construction. Figures 12 and 13 show the axial force distributions and maximum axial forces of the columns in the subway station, which can be used to understand the variation trend of the axial force of the columns in the subway station after foundation pit excavation. Figures 12 and 13 show that the axial forces of the columns in the subway station were evenly distributed and under pressure. The column pressure was the smallest at the end of the station far from the foundation pit, and the column bottom pressure was the largest at the middle of the station. Additionally, as foundation pit excavation progressed, the maximum axial force of the station column increased from 12357.06 kN before excavation to 13639.25 kN after excavation, increasing by 10.38%. During foundation pit construction, attention should be given to the stress change of the station column, especially the stress at the bottom of the column in the middle of the station, and dynamic monitoring should be performed at all times to prevent accidents [14].

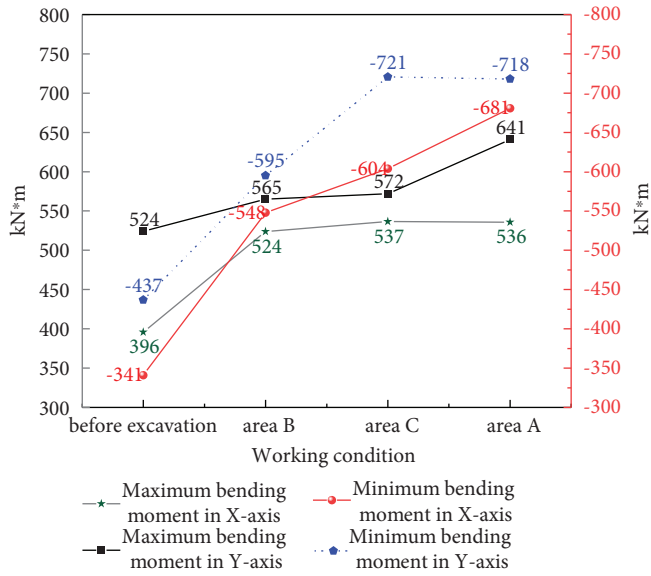

Figure 10: Maximum bending moment of the common diaphragm wall from the foundation pit excavation to the pit bottom.

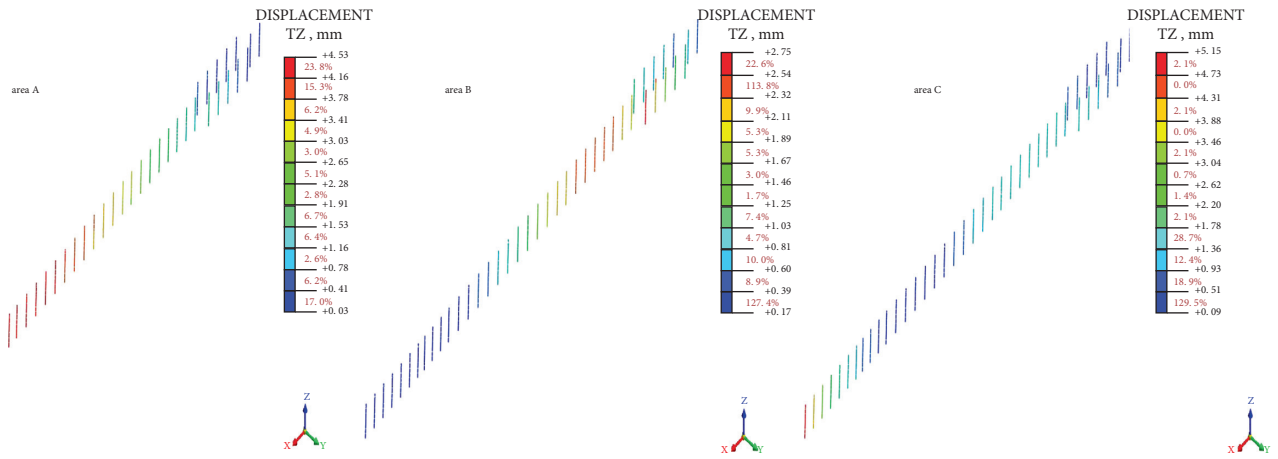

Figure 11: Vertical displacement of the station column from the foundation pit excavation to the pit bottom in each area.

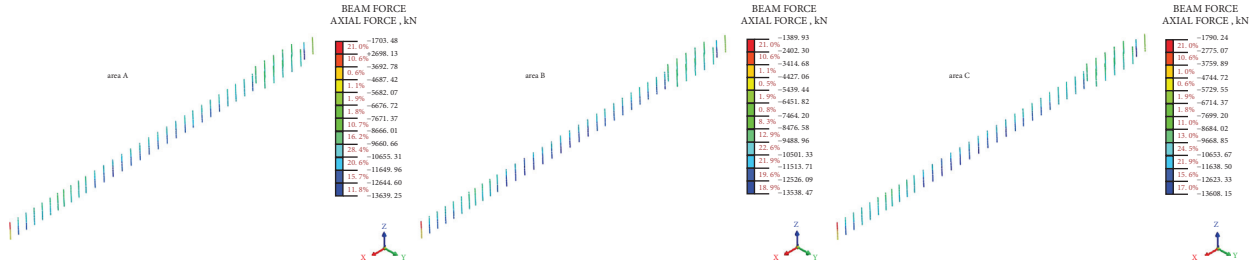

Figure 12: Axial diagram of the station column from the foundation pit excavation to the pit bottom in each area.

5. Analysis of the Influence of the Foundation Pit Retaining Structure on the Station

5.1. Analysis of the Influence of the Foundation Pit Enclosure Structure Thickness. Retaining structures with different thicknesses have various effects on foundation pit deformation [15]. The diaphragm wall of the existing station structure was 0.8 m thick. To explore the influence of the thickness of the newly built diaphragm wall of the deep foundation pit, which shares a diaphragm wall with the existing subway station, on the existing station structure, the deformations of the subway station bottom plate were

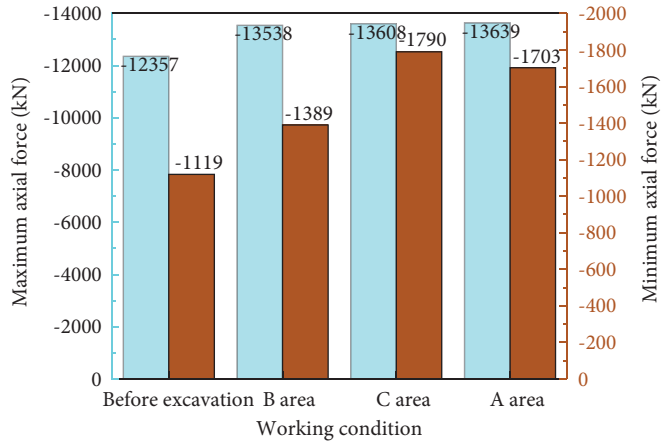

Figure 13: Maximum axial force of the station column during foundation pit excavation.

compared for eight thicknesses of 0.4 m, 0.6 m, 0.8 m, 1.0 m, 1.2 m, 1.4 m, 1.6 m, and 1.8 m with a three-dimensional model of condition 2. Figure 14 shows the horizontal and vertical displacement diagrams of the station bottom plate near the foundation pit when the foundation pit was excavated with different thicknesses. Figure 14 shows that when the thickness of the new diaphragm wall was less than that of the existing diaphragm wall, the vertical deformation of the station bottom plate first increased and then decreased with increasing thickness. When the thickness of the new diaphragm wall exceeded the thickness of the existing diaphragm wall, the vertical deformation of the station bottom plate also first increased and then decreased with increasing thickness. When the thickness exceeded 1.0 m, the reduction trend of the vertical deformation of the station bottom plate gradually slowed, and increasing the thickness of the new diaphragm wall only increased the cost and had a poor effect. When the thickness of the new diaphragm wall was 0.4 m, the vertical deformation of the station bottom plate was 7.13 mm. When the thickness of the new diaphragm wall was 0.8 m, that is, when the thickness of the new diaphragm wall was the same as that of the existing diaphragm wall, the vertical deformation of the station bottom plate was 7.09 mm. When the two thicknesses are compared, they are very similar. The author believes that the main reason for this is that the thickness of the new diaphragm wall was half the thickness of the existing diaphragm wall. In addition to resisting the deformations caused by foundation pit excavation, the Earth pressure at the bottom of the new diaphragm wall was small and less affected by the uplift of the pit bottom soil.

When the thickness of the new diaphragm wall exceeded the thickness of the existing diaphragm wall, the horizontal deformation of the station bottom plate gradually increased with increasing thickness because there was a difference in the stiffness of the retaining structure on both sides of the foundation pit. As the thickness of the diaphragm wall increased, the stiffness of the retaining structure of the foundation pit increased. After earthwork excavation and unloading, areas of the retaining structure with high stiffnesses had a strong resistance to deformation. The whole

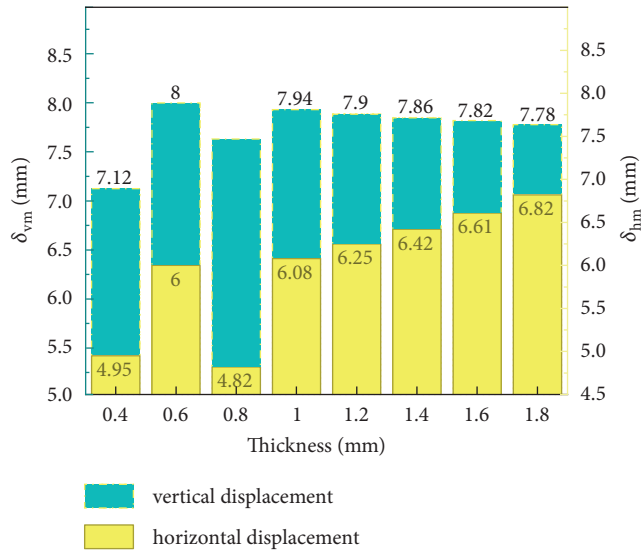

Figure 14: Horizontal and vertical displacements of the station floor near the foundation pit.

foundation pit was offset to the side due to the high stiffness of the foundation pit retaining structure, which increased the horizontal deformation of the existing station structure [16]. In summary, without considering other factors, the thickness of the new diaphragm wall should be the same as that of the existing diaphragm wall or half the thickness of the original diaphragm wall.

5.2. Analysis of the Influence of the Depth of the Foundation Pit Retaining Structure. The burial depth of the diaphragm wall has a great influence on its stiffness and bending moment, as well as the stability of the foundation pit support system [17]. When the diaphragm wall is at an insufficient depth, the supporting structure has an insufficient strength, resulting in instability and endangering the foundation pit and surrounding environment [18]. When the thickness of the diaphragm wall is known, increasing its depth can reduce the wall displacement and the uplift resistance of the soil at the

Table 4: Simulation conditions of foundation pit excavation with different depths of the diaphragm wall.

Working condition	1	2	3	4	5	6	7	8	9	10
Depth (m)	20.34	22.60	25.11	27.90	31.00	34.10	37.51	41.26	45.39	49.93

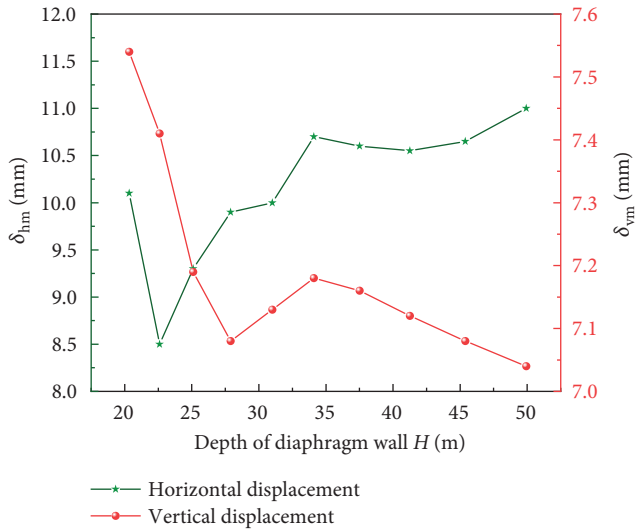

Figure 15: Vertical and horizontal displacements of the station floor structure near the foundation pit.

bottom of the foundation pit, but blindly increasing its depth increases the cost of the support structure. To explore the influence of the depth of the newly built diaphragm wall of the deep foundation pit, which shares a diaphragm wall with the existing subway station, on the structure of the existing station, a three-dimensional model of condition 2 was used, with gradual increases or decreases of 10% of the depth of the existing diaphragm wall. Ten different depth conditions were selected, as shown in Table 4.

Figure 15 shows the vertical and horizontal displacements of the station slab near the foundation pit when the foundation pit was excavated to the bottom under different working conditions. As the depth of the new diaphragm wall was gradually increased, when the depth of the new diaphragm wall exceeded the depth of the existing station diaphragm wall, the vertical deformation of the existing subway station increased slightly and then decreased gradually when the depth was increased by 10%. Before the depth of the diaphragm wall of the existing subway station was exceeded, the vertical displacement of the station first decreased and then increased slightly with as the depth of the diaphragm wall increased, and the relative horizontal deformation of the station slab first decreased and then increased with increasing depth. When the depth of the new ground wall was small, the stability of the foundation pit was poor [19]. With increasing depth, the overall stability of the foundation pit retaining structure improved. Moreover, the difference between the depth of the old and new ground connecting walls caused the embedded soil of the two deep foundation pits to differ. Furthermore, the Earth pressure behind the wall varied considerably. As the depth of the ground connecting wall increased, the active Earth pressure behind the ground connecting wall increased, posing a great challenge to the stability of the foundation pit.

6. Conclusions

Based on a deep foundation pit project in Suzhou, a numerical simulation analysis of a deep foundation pit adjacent to a subway station was performed, the deformation and stress of the subway station structure after the construction of a deep foundation pit was studied, and the influence of the foundation pit retaining structure on the station was analyzed. The following conclusions were reached:

(1) During the foundation pit excavation process, the subway station slab rose as a whole and was greatly affected by the deformation of the common ground connecting wall. The most unfavorable position shifted as the excavation area changed, mainly on the side of the common ground connecting wall. The foundation pit excavation had little effect on the bending moment of the station floor, but the floor near the wall produced a negative bending moment, which may cause cracking.

(2) The deformation trend of the station wall was the same as that of the station slab. The bottom of the station wall near the excavation area displaced into the foundation pit, the middle and upper parts of the wall and the east and west ends deformed outside the foundation pit, and the common ground connecting wall bulged upward as the foundation pit was excavated. However, there was little impact on the bending moment on the wall. The excavation of the foundation pit in different zones had little effect on the displacement of the common diaphragm wall of the foundation pit in the east-west direction, but it had a great effect on the east-west displacement of the common diaphragm wall outside the foundation pit. The stress on the common diaphragm wall changed greatly before and after excavation. The positive bending moment in the X direction increased by 35.29%, while the negative bending moment increased by 99.71%. The positive bending moment in the Y direction increased by 22.26%, while the negative bending moment increased by 64.44%. Overall, foundation pit excavation has a great impact on the negative bending moment of the common diaphragm wall. In the design of similar projects, the negative reinforcement configuration of the common diaphragm wall should be considered.

(3) During the foundation pit excavation process, the subway station column lifted upward, and the maximum displacement, which was located at the west end of the station near the foundation pit,

gradually weakened from west to east. As the foundation pit excavation process continued, the maximum axial force of the station column increased by 10.38%, and the pressure was the largest at the bottom of the middle column. Dynamic monitoring should be carried out to prevent accidents.

(4) As the thickness of the diaphragm wall increased, the stiffness of the foundation pit retaining structure increased. After earthwork excavation and unloading, areas of the retaining structure with a high stiffness could resist deformations. The whole foundation pit was offset to the side due to the high stiffness of the foundation pit retaining structure, increasing the horizontal deformation of the existing station structure. With increasing thickness, the relative horizontal deformation of the station slab gradually increased, mainly because the difference in the depths of the old and new diaphragm walls caused the embedded soil at the base of the two deep foundation pits to differ. Furthermore, there was a great difference in the Earth pressure behind the wall. As the depth of the diaphragm wall increased, the active Earth pressure behind the diaphragm wall increased.

Data Availability

The data (experimental results) used to support the findings of this study are included in the article.

Conflicts of Interest

The authors declare that there are no conflicts of interest regarding the publication of this paper.

Acknowledgments

The authors would like to thank AJE (https://www.aje.cn) for English language editing. This work was supported by the Key Research and Development Project of Shaanxi Province (No. 2021SF-523).

References

[1] Z. Ding, J. Jin, and T.-C. Han, "Analysis of the zoning excavation monitoring data of a narrow and deep foundation pit in a soft soil area," *Journal of Geophysics and Engineering*, vol. 15, no. 4, pp. 1231–1241, 2018.

[2] S. H. Ye, Z. F. Zhao, and D. Q. Wang, "Deformation analysis and safety assessment of existing metro tunnels affected by excavation of a foundation pit," *Underground Space*, vol. 6, no. 4, pp. 421–431, 2020.

[3] J. Y. Chun, *Study on Deformation Estimation of Soft Soil Foundation Pit and its Influencing Factors*, Hohai University, Nanjing, China, 2001.

[4] L. Z. Sun, "Influence analysis of foundation pit excavation on adjacent metro station," *Special Structures*, vol. 33, no. 6, pp. 52–55, 2016.

[5] Q. Wang, H. Qian, and Q. Qian, "Analysis of impact of bilateral deep foundation pit excavation on adjacent existing station," *IOP Conference Series. Earth and Environmental Science*, vol. 252, no. 5, Article ID 52049, 2019.

[6] H. Z. Guo and C. R. Bai, "Key technology analysis of shield tunneling in Luobao section of Shenzhen Metro line 13," *Modern Tunnel Technology*, vol. 57, no. S1, pp. 951–956, 2020.

[7] H. Liu, K. Li, J. Wang, and C. Cheng, "Numerical simulation of deep foundation pit construction under complex site conditions," *Advances in Civil Engineering*, vol. 2021, Article ID 6669466, 11 pages, 2021.

[8] Z. Hu, Q. Wang, S. Yang et al., "Numerical simulation of soil displacement and settlement in deep foundation pit excavations near water," *Geofluids*, vol. 2021, Article ID 5559009, 14 pages, 2021.

[9] *Technical Code for Construction Safety of Deep Foundation Pit Engineering*, China, 2013.

[10] S. Y. Fan, Z. P. Song, T. Xu, K. M. Wang, and Y. W. Zhang, "Tunnel deformation and stress response under the bilateral foundation pit construction: a case study," *Archives of Civil and Mechanical Engineering*, vol. 21, no. 3, pp. 1–19, 2021.

[11] X. Zhang, G. Wei, and C. Jiang, "The study for longitudinal deformation of adjacent shield tunnel due to foundation pit excavation with consideration of the retaining structure deformation," *Symmetry*, vol. 12, no. 12, p. 2103, 2020.

[12] C. S. Luo, Y. H. Cheng, Z. Bai, T. Shen, X. Y. Wu, and Q. G. Wang, "Study on settlement and deformation of urban viaduct caused by subway station construction under complicated conditions," *Advances in Civil Engineering*, vol. 2021, Article ID 6625429, 16 pages, 2021.

[13] H. Xing, F. Xiong, and J. Wu, "Effects of pit excavation on an existing subway station and preventive measures," *Journal of Performance of Constructed Facilities*, vol. 30, no. 6, Article ID 04016063, 2016.

[14] H. J. Zhao, W. Liu, P. X. Shi, J. T. Du, and X. M. Chen, "Spatiotemporal deep learning approach on estimation of diaphragm wall deformation induced by excavation," *Acta Geotechnica*, vol. 16, no. 11, pp. 1–15, 2021.

[15] M. N. Houhou, F. Emeriault, and A. Belounar, "Three-dimensional numerical back-analysis of a monitored deep excavation retained by strutted diaphragm walls," *Tunnelling and Underground Space Technology*, vol. 83, pp. 153–164, 2019.

[16] J. Wang, H. Xiang, and J. Yan, "Numerical simulation of steel sheet pile support structures in foundation pit excavation," *International Journal of Geomechanics*, vol. 19, no. 4, Article ID 05019002, 2019.

[17] C.-F. Zeng, X.-L. Xue, and M.-K. Li, "Use of cross wall to restrict enclosure movement during dewatering inside a metro pit before soil excavation," *Tunnelling and Underground Space Technology*, vol. 112, Article ID 103909, 2021.

[18] C. G. Zhang, X. D. Chen, and W. Fan, "Overturning stability of a rigid retaining wall for foundation pits in unsaturated soils," *International Journal of Geomechanics*, vol. 16, no. 4, Article ID 6015013.1, 2016.

[19] X. Wang, Q. Song, and H. Gong, "Research on deformation law of deep foundation pit of station in core region of saturated soft loess based on monitoring," *Advances in Civil Engineering*, vol. 2022, Article ID 7848152, 16 pages, 2022.